Compact Broadband Wavelength Selective Switch based on In-fiber Diffraction Device

Qingguo Song, Yuze Dai, Xiangpeng Xiao, Haoshuo Chen, Chen Liu, Xuewen Shu, Qizhen Sun, Kaiming Zhou, Lin Zhang, Zhujun Wan and Zhijun Yan

***Abstract*— In this study, a compact and broadband wavelength selective switch (WSS) based on a radiated tiled fiber grating with 45 ° tilt angle (RTFG) is proposed and experimentally demonstrated. The 45 ° RTFG is employed as both radiating and receiving light, replacing the fiber arrays and bulky dispersion element in the traditional WSS system. We have theoretically and experimentally investigated the proposed WSS in terms of operating wavelength range, spectral resolution and insertion loss. In the experiment, a 1×2 compact WSS based on 45 ° RTFG and LCoS is achieved, which has a wide operation range between 1520nm and 1597nm, covering the C+L bandwidth. The measured spectral resolution and tuning accuracy are 0.4nm and 0.08nm, respectively. The insertion loss of the WSS system is about 20 dB, which is mainly caused by the aperture loss of 45 ° RTFG. Moreover, we have also investigated the spectral filtering performance of the proposed WSS, in which the filtered spectral of the channel spacing of 300GHz, 200GHz and 100GHz are realized. The proposed in-fiber 45° RTFG diffraction device based WSS has a compact structure and C+L covered bandwidth, which can be potentially used for optical fiber communication.**

***Index Terms*—fiber gratings, wavelength selected switch**

I. Introduction

With the rapid development of the internet and artificial intelligence, there is a growing demand for increasing the optical communication network bandwidth. Different optical signal processing technologies have been developed to increase the capacity of optical communications such as optical time-division multiplexing (OTDM) [1], polarization-division multiplexing (PDM) [2] and dense wavelength division multiplexing (DWDM) [3]. With the development of the high speed and large capacity data transmission technology, signal switching which is efficient and compact in all-optical networks becomes more and more important. Reconfigurable Optical Add/Drop Multiplexer (ROADM), which can achieve the remote switching of wavelengths through the intersections of DWDM networks, has been gradually used to replace the traditional electric switches due to its high efficiency and flexibility [4-8]. Wavelength selective switch (WSS) is the key component in ROADM systems, which can realize the signal switching of any wavelength channel from a common port to different output ports. So far, various types of technology for WSS have been reported, including Microelectromechanical Mirrors (MEMS) [9], Liquid Crystal (LC) [10] on glass and Liquid Crystal on Silicon (LCoS) [11-12]. Among these technologies, the LCoS phase array with millions of pixels that can approximate steering mirrors through blazed phase gratings support is more suitable for flexible grid WSS due to the high port counts and high reliability. For common WSS, the end face of the optical fiber is used as the element that emits and receives spatial beams, and a bulk diffraction grating is used for separating beams of different wavelengths in space [13]. The complex system and large volume are the limitations of its application in optical communication. To develop integrated optical devices and systems, it is necessary to design miniaturized. A multiple-stacked arrayed waveguide grating (AWG) for LCoS-based WSS is proposed, which can be used as a wavelength multiplex/demultiplexer replacing the bulk diffraction grating [14]. The AWG-based WSS has a simpler configuration with less bulky components, but the operation spectral range is only ~25nm.

Recently, radiated tiled fiber grating (RTFG) has been used as an ideal all-fiber polarizer and all-fiber diffraction device [15-16] due to its unique polarization-dependent mode coupling characteristics. The RTFG can radiate the core mode out of fiber with a wavelength-dependent angle [17]. Based on its radiation and diffraction characteristics, the RTFG can replace bulk diffraction grating in spectral related applications [18], which has been applied to compact linear polarization spectrometers [19], highly efficient spectrally encoded imaging systems [20] and optical time stretching imaging systems [21]. Recently, A highly efficient coupler to access remotely placed optical fiber sensor based on 45 ° RTFG grating is proposed [22], in which the 45 ° RTFG can transmit and receive light simultaneously as a free-space fiber coupler.

In this paper, we proposed a compact WSS based on 45 ° RTFG which supports broadband operation covering the C+L band. The proposed WSS has a direct dispersion interface, in which the 45 ° RTFG is employed as both the diffractive and beam coupling device, replacing

This work was supported in part by the National Natural Science Foundation of China (No. 62075071), the National Key Research and Development Program of China (2023YFE0105800), the National Science Fund for Excellent Young Scholars (No. 61922033). (*Corresponding author: Zhijun Yan and Zhujun Wan*)

Qingguo Song, Yuze Dai, Xiangpeng Xiao, Chen Liu, Qizhen Sun, Zhujun Wan and Zhijun Yan are with the School of Optical and Electronic Information, National Engineering Laboratory for Next Generation Internet Access System, Huazhong University of Science and Technology, Wuhan 430074, China, and also with the Wuhan National Laboratory for Optoelectronics, Huazhong University of Science and Technology, Wuhan 430074, China. (e-mail: D202180835@hust.edu.cn; u201713799@hust.edu.cn; xpxiao@hust.edu.cn; liuchen@hust.edu.cn; qz_sun@hust.edu.cn; zhujun.wan@hust.edu.cn; yanzhijun@hust.edu.cn).

Haoshuo Chen is with the Nokia Bell Labs, 791 Holmdel Rd., Holmdel, New Jersey 07733, USA (e-mail: haoshuo.chen@nokia-bell-labs.com).

Kaiming Zhou and Lin Zhang is with the Aston Institute of Photonic Technologies, Aston University, Birmingham, B4 7ET, UK.T. C. (e-mail: k.zhou@aston.ac.uk; l.zhang@aston.ac.uk).

the fiber arrays and bulky dispersion element in the traditional WSS system. The RTFGs are inscribed in the single mode fiber (SMF) by UV exposure and integrated into an array, in which every RTFG can be used as input and output ports at the same time. Furthermore, the bandwidth and resolution of the RTFG-based WSS have been experimentally investigated. The compact structure and C+L covering bandwidth of the proposed WSS make it potential for integrated ROADM systems.

II. Device Principle and Theoretical Analysis

The 45 ° RTFG is an ideal in-fiber diffraction device. Fig.1(a) illustrates the diffraction characteristics of 45 ° RTFG, in which the core mode of fiber will be radiated into free space with a wavelength-dependent emission angle θ. The relationship between the diffraction angle θ and the wavelength λ is experimentally measured as shown in Fig.1(b), in which the wavelength range is 1480~1640 nm and the angular dispersion is 0.053 °/nm. Owing to the special inclined grating structure, the emission light has a divergence azimuth φ at the x-direction, as seen in Fig.1(c). In order to collect the energy of the divergent beam, the microlens are used to collimate the beam. The radiation energy dispersion of 45° RTFG is measured, in which the distribution of the collimated beam is quasi-Gaussian, as seen in Fig.1(d).

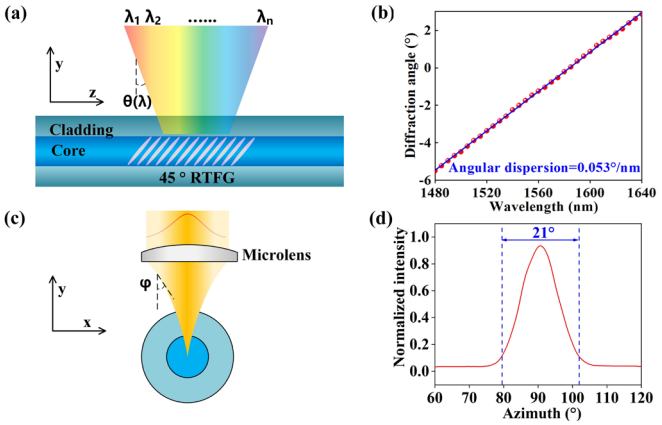

Fig.1 (a) The diagram of the diffraction characteristics of 45 °RTFG. (b)The angular dispersion of 45 ° RTFG; (c) Radiation beam divergence in the radial direction. (d) The radiation energy distribution in the x-y plane.

The principle of the WSS based on RTFG is shown in Fig.2, in which the axial direction of the optical fiber corresponds to the z-direction and the direction of the emitted light corresponds to the y-direction. In the horizontal direction (y-z plane), the transmission light of fiber is diffracted into free space by the 45 ° RTFG, thereafter the diffracted light is focused by a horizontal lens on a liquid crystal on silicon (LCoS). The focusing spots of different wavelengths are separated spatially and correspond to different pixels in LCoS. 45 ° RTFGs with the same structural parameters are placed parallelly in the vertical direction (x-z plane), and a cylindrical lens (CL) array is employed to collimate or focus the beam. The focused beam after a vertical lens is steered by the LCoS, and then recoupled by other 45 ° RTFG ports.

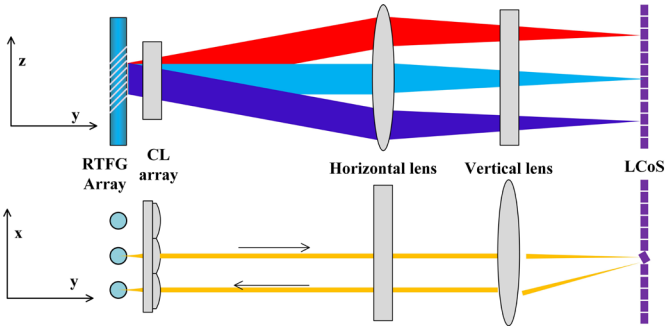

Fig.2 The principle of WSS based on 45° RTFG

The spectral distribution $I_{out}(\lambda)$ of the output light can be expressed as:

$$I_{out}(\lambda) = I_{in}(\lambda) \cdot T(\lambda)T'(\lambda)S(\lambda)A(\lambda) \quad (1)$$

Where $I_{in}(\lambda)$ is the spectral distribution of input light. $T(\lambda)$ and $T'(\lambda)$ are the radiating and recoupling efficiency between the fiber core and free space respectively. $S(\lambda)$ is the wavelength modulation function of LCoS. $A(\lambda)$ is the function of operating range.

In our previous work, the radiating efficiency $T(\lambda)$ has been theoretically analyzed using a segmental method [23]. The radiation of RTFG is a serial process, in which the transmission light goes through each grating segment in sequence. By contrast, the recoupling of RTFG is a parallel process, in which the light is coupled by all grating segments simultaneously. The T and T' can be expressed as:

$$\begin{cases} T = \alpha_R(1-\alpha_R)^m \\ T' = m\alpha_R \end{cases} \quad (2)$$

Where α_R is the coupling efficiency of a single grating segment, and m is the number of segments. The α_R is related to the polarization state δ, azimuth φ of the coupling light and wavelength λ. The wavelength modulation function $S(\lambda)$ is determined by the phase blazed grating loaded on the LCoS, which can be the coding function of arbitrary distribution. By converting the modulation function into the influence of azimuth deflection on coupling efficiency. The first three items of equation (1) can be expressed as:

$$T(\lambda)T'(\lambda)S(\lambda) = m\alpha_R^2(\lambda, \varphi - \varphi_s(\lambda)) \cdot [1-\alpha_R(\lambda, \varphi - \varphi_s(\lambda))]^m \quad (3)$$

Where $\varphi_s(\lambda)$ is the azimuth of deflection after the lens system and LCoS, which is given by:

$$\varphi_s(\lambda) = \frac{d - f_V \cdot \varphi_{LCoS}(\lambda)}{f_M} \quad (4)$$

Where d is the interval of the adjacent microlens, f_M is the focal length of the microlens, f_V is the focal length of the vertical lens, $\varphi_{LCoS}(\lambda) = arcsin[\frac{\lambda}{M(\lambda)d}]$ is the deflection angle caused by LCoS, in which d is the pixel size and $M(\lambda)$ is phase grating period at corresponding wavelength.

The working bandwidth is determined by the grating length, lens aperture and focal length of the lens. As shown in Fig.3(a), the size of the radiated beam is the same as the length of the grating. According to our previous research, the radiated beam has an energy distribution that decays exponentially along the axis. After the horizontal lens and LCoS, an apart energy will be lost during the recoupling process due to the beam deflection.

The beam with a larger diffraction angle has a larger beam deflection, which limits the operating bandwidth of the WSS. Although the position of another RTFG during recoupling can be adjusted to change the working wavelength, the maximum working bandwidth is fixed. The function of working bandwidth can be expressed as:

$$A(\lambda) = \frac{\int_0^{2L-H(\lambda)+D} \beta dz}{\int_0^L e^{-\alpha z} dz} = \frac{\beta[2L-H(\lambda)+D]}{e^{-\alpha L}-1} \quad (5)$$

Where L is grating length. D is the mismatch between the radiating and recoupling RTFG at the horizontal direction. $H(\lambda)$ is the maximum distance of the light deflection, which is given by:

$$H(\lambda) = 2f_H \cdot tan[arcsin(\frac{L}{2r}) - \frac{arcsin(\frac{L}{2r})-\theta(\lambda)}{n}] \quad (6)$$

Where f_H is the focal length of the horizontal lens. $\theta(\lambda)$ is the diffraction angle of different wavelengths, which can be obtained by the phase matching condition.

According to equation (1-6), the working bandwidth of the proposed LCoS can be theoretically analyzed, which is shown in Fig.3(b), the wavelength range can be adjusted by changing the mismatch D between the radiating and recoupling RTFG.

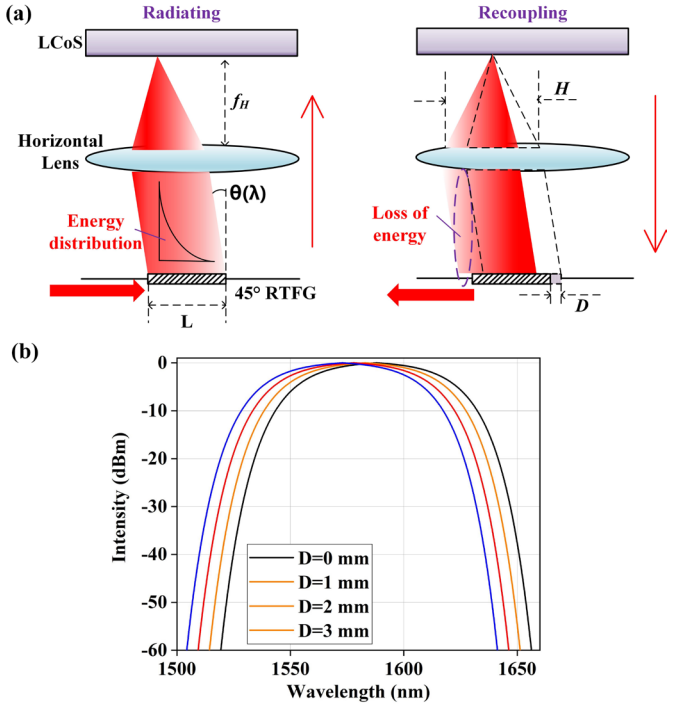

Fig. 3 (a)The diagram of the radiating and recoupling process. (b)The Simulation of operation bandwidth of WSS at different positions of recoupling RTFG.

III. Experimental Results And Discussion

For the traditional WSS system, a bulk diffraction grating is used for the dispersion of light, which can be replaced by the RTFG. A 1×2 WSS based on 45 ° RTFG is set, where the schematic is shown in Fig.4(a), and the associated experimental setup is given in Fig.4(b). The 45° RTFGs are inscribed in the SMF using the UV-exposure method, which has a grating period of 788 nm, corresponding to a broad radiation wavelength range of 300nm [23]. The light from a broadband light source is transmitted in the fiber core and radiated by a 45 ° RTFG. The radiated light has a divergence angle in the vertical direction, which is collimated by a cylindrical lens array with a focal length of 1mm. Then the collimated light is focused by two orthogonal cylindrical lenses, and incident to an LCoS (HAMAMATSU, X15223) which has a screen pixel of 1280×1024 and a pixel size of 12.5 μm. The focal lengths of CL1 and CL2 are 200 mm and 150 mm respectively. Spectral switching and filtering can be realized by loading phase grating on LCoS. The modulated light is recoupled by a 45 ° RTFG array, which is fixed on a plate with V-groove, the V-groove has the same pitch as the CL array of 300 μm. The filtered spectrum is observed by an optical spectrum analyzer (OSA). Especially, the radiated light from the RTFG has a single S-polarization state, which corresponds to the response polarization of the LCoS.

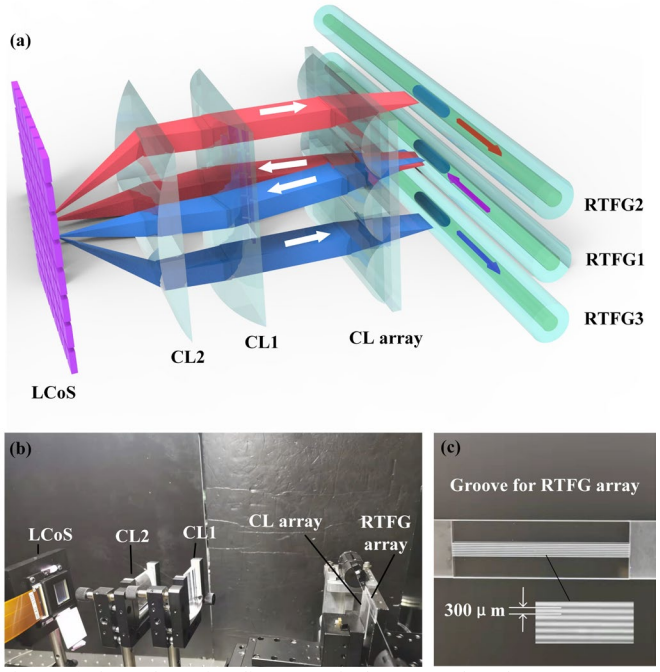

Fig.4 (a)The schematic diagram of the WSS based on 45 ° RTFG. (b)Experimental setup. (c) The groove for the RTFG array

A broadband light source with a bandwidth of 1400nm~1700nm is incident to the input port (RTFG1). The spectra of the input and output ports are measured. As shown in Fig.5, the wavelength range of the output is 77 nm (1520~1597 nm), covering the C band and a part of the L band. The unevenness of the spectra is mainly due to the original spectra of the source. And the bandwidth of WSS is limited by the size of LCoS (1280×12.5um=16mm), in which the linear dispersion of the diffracted light is 0.185 mm/nm at the focal lengths of 200 mm, leading to a theoretical maximum wavelength range of 86nm. The loss of the WSS is about 20dB, which is mainly caused by the low recoupling efficiency of 45° RTFG. Table.1 shows the specific loss of the proposed WSS. The 45° RTFG has a single polarization-dependent radiation property, and for the broadband light, half of the energy will remain in the fiber as transmitted light, which leads to a 3dB polarization coupling loss. There is a loss caused by the fiber connector of 1dB, LCoS and lens of 2dB, which can be optimized by changing the

optical components. The recoupling of 45° RTFG leads to a loss of 14dB, which is the main loss of the whole WSS system. When the reflected light returns to the grating and recouples into the fiber, the energy will distribute on various grating cross-sections, leading to a low recoupling efficiency. The loss of the WSS system can be reduced by exchanging the LCoS and lens system with less optical loss. The recoupling efficiency of 45° RTFG can be improved by increasing the diameter of the fiber core or increasing the refractive index modulation depth of grating.

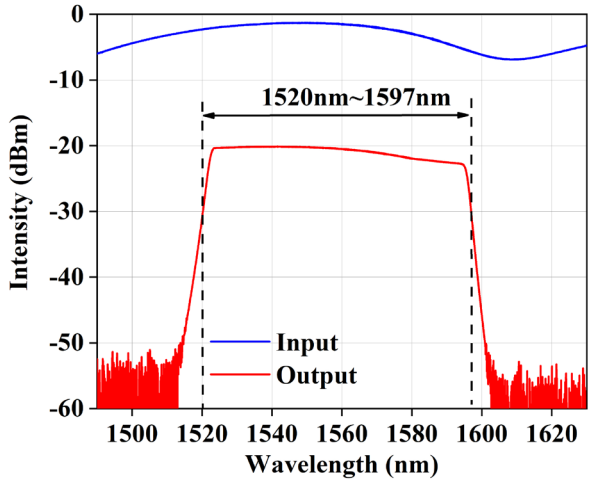

Fig.5 The bandwidth of the RTFG-based WSS

Table.1 The Loss of the WSS based on 45° RTFG

Category	Loss
Polarization coupling loss	3dB
Fiber connector	1dB
LCoS and Lens	2dB
recoupling loss	14dB
Total	20dB

The spectral tuning accuracy can be expressed as the optical wavelength covered on a single pixel of the LCoS:

$$R = d_{LCOS}\frac{\partial\lambda}{\partial y} \tag{7}$$

Where d_{LCOS} is the size of a single pixel of LCoS. $\frac{\partial\lambda}{\partial y}$ is the reciprocal of the linear dispersion rate of 45°RTFG [16], which is given by:

$$\frac{\partial\lambda}{\partial y} = \frac{f_H n^2 \Lambda}{(1+(\cot\theta-\frac{n\Lambda}{\lambda\sin\theta})^2)\lambda^2\sin\theta}\cdot\frac{1}{\sqrt{1+(1-n^2)(\cot\theta-\frac{n\Lambda}{\lambda\sin\theta})^2}} \tag{8}$$

By moving the pixel of the loaded phase grating of LCoS, the spectral resolution and tuning accuracy of the WSS system can be investigated. In this work, the channel spacing of the input light is set to 100 Ghz. The width and period of loaded phase grating are 8 pixels and 12 pixels respectively. As shown in Fig.6, the 3dB bandwidth of the filtered signal is 0.4 nm and the spectral tuning accuracy is 0.08 nm. Especially, the loss of WSS will surge when the number of pixels is less than 8, which is caused by the low recoupling efficiency of RTFG. And the resolution can be improved by designing the structure of RTFG with higher dispersion and recoupling efficiency.

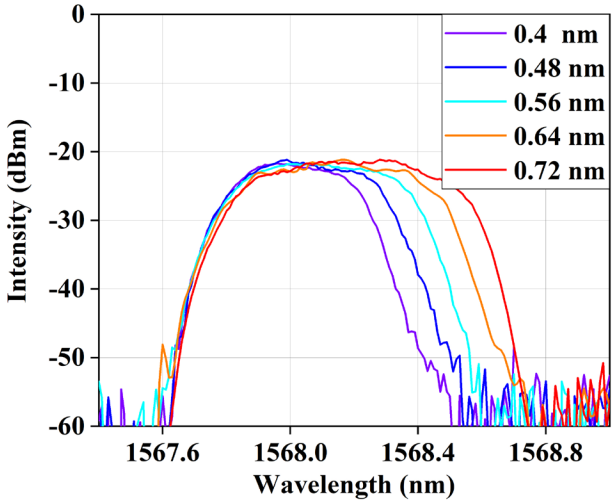

Fig.6 The resolution of the RTFG-based WSS

To evaluate the wavelength selective performance of the proposed WSS based on the 45° RTFG, the periodic phase gratings with different interleaved patterns are loaded on the LCoS. Fig.6 gives a steering pattern on the LCoS, the intensity of channel can be adjusted by changing the initial phase of phase grating. Fig.7 gives pattens the output spectral with the channel spacing of 300GHz, 200GHz and 100GHz. The working bandwidth covers 1525 nm to 1595 nm. Especially, when the channel spacing is 100GHz, there is a tendency to overlap of some adjacent channels, which is caused by the gentle roll-off of some channels. The roll-off can be steeped by exchanging the LCoS with a smaller pixel size. The experimental result shows that the WSS based on 45° RTFG has an ideal wavelength selective performance within the C+L band.

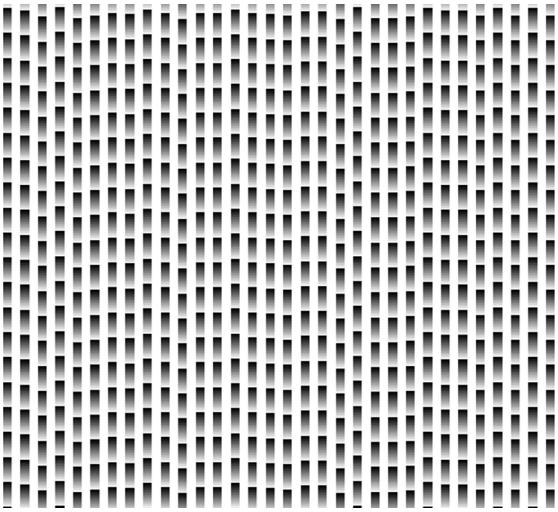

Fig.7 Steering pattern on the LCoS

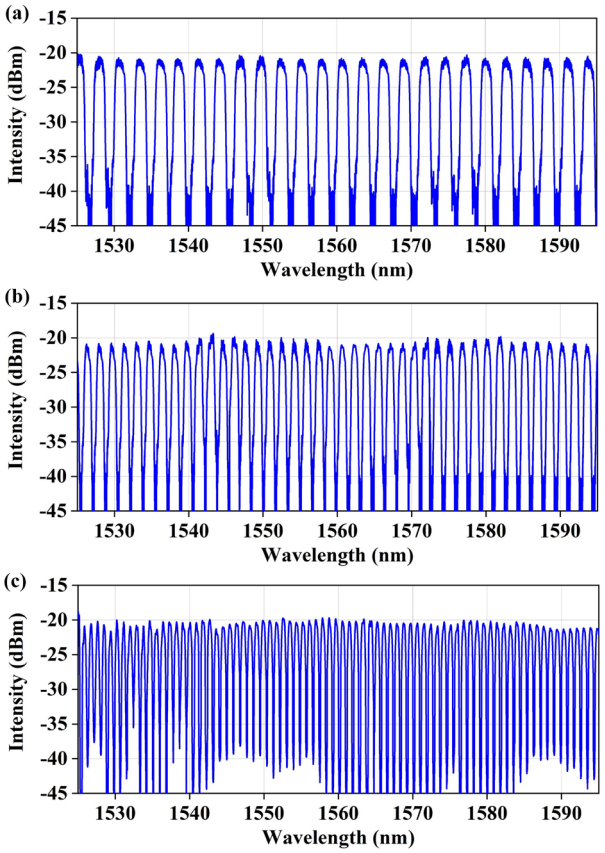

Fig.8 Output spectral with the channel spacing of (a) 300GHz, (b) 200GHz and (c) 100GHz.

Due to the high polarization dependent radiation property of 45° RTFG and the polarization sensitivity of LCoS, the proposed WSS system is only working with S-polarization. For the traditional WSS system, the polarization beam splitters and waveplates could be employed to solve the polarization dependent issue in [11]. In our recent work, we have used a coated 45 ° RTFG and cascaded Faraday Rotator Mirror (FRM) structure to realize the simultaneous radiation of the incident light with different polarization states [24], in which the emission RTFG is half-coated with a gold film, the S-polarization light would be diffracted out from the fiber, and the P-polarization light was transmitted through the grating and reflected at the Faraday Rotator Mirror (FRM). The reflected light would experience the polarization rotation effect and become backwards-propagating S-polarization light, which will be diffracted by the RTFG in another direction, finally reflected by the gold film and emitted from the fiber with the forward-propagating S-polarization light. By cascading an FRM, the proposed WSS system could potentially reduce the polarization dependent loss to a very low level.

IV. CONCLUSION

In conclusion, we have theoretically and experimentally demonstrated an WSS based on an in-fiber 45° RTFG diffraction device. The in-fiber transmission light is diffracted out of the side of fiber by a 45° RTFG with a wavelength-dependent emission angle. The operating wavelength range of the proposed WSS is working at the wavelength range between 1520 nm and 1597 nm, which covers the C+L band. The spectral resolution and tuning accuracy is measured of 0.4 nm and 0.08 nm, respectively. The insertion loss of the WSS system is about 20 dB, which is mainly caused by the aperture loss of 45 ° RTFG. Moreover, we have also investigated the spectral filtering performance of the proposed WSS, in which the signal spectra with channel spacing of 200GHz, 100GHz and 50GHz are measured.

REFERENCES

[1] Masato Yoshida, Kosuke Kimura, Taro Iwaya, Keisuke Kasai, Toshihiko Hirooka, and Masataka Nakazawa, "Single-channel 15.3 Tbit/s, 64 QAM coherent Nyquist pulse transmission over 150 km with a spectral efficiency of 8.3 bit/s/Hz,". Optics Express, vol. 27, no. 12, pp. 28952-28967, 2019.

[2] J. Yang, E. Sillekens, W. Yi, P. Bayvel, and R. I. Killey, "Joint estimation of dynamic polarization and carrier phase with pilot-based adaptive equalizer in PDM-64 QAM transmission system," Optics Express, vol. 29, no. 26, pp. 43136-43147, 2021.

[3] M. Schädler, G. Böcherer, F. Pittalà, S. Calabrò, N. Stojanovic, C. Bluemm, M. Kuschnerov, and S. Pachnicke, "Recurrent Neural Network Soft-Demapping for Nonlinear ISI in 800Gbit/s DWDM Coherent Optical Transmissions," Journal of Lightwave Technology, vol. 39, no. 16, pp. 5278-5286, 2021.

[4] Y. Pointurier et al., "Analytical study of crosstalk propagation in all-optical networks using perturbation theory," Journal of Lightwave Technology, vol. 23, no. 12, pp. 4074–4083, Dec. 2005.

[5] N. Kataoka et al., "Field trial of 640-Gbit/s- throughput, granularity flexible optical network using packet-selective ROADM prototype," Journal of Lightwave Technology, vol. 27, no. 7, pp. 825–831, Apr. 2009.

[6] S. Tibuleac et al., "Transmission impairments in DWDM network with reconfigurable optical add–drop multiplexers," Journal of Lightwave Technology, vol. 28, no. 4, pp. 557–568, 2010.

[7] Y.-T. Hsueh et al., "Passband narrowing and crosstalk impairments in ROADM-enabled 100G DWDM networks," Journal of Lightwave Technology, vol. 30, no. 24, pp. 3980–3986, 2012.

[8] C. Vagionas, A. Tsakyridis, T. Chrysostomidis, I. Roumpos, K. Fotiadis, A. Manolis, J. Mu, M. Dijkstra, S. Garcia Blanco, R. M. Oldenbeuving, P. W. L. van Dijk, C. G. H. Roeloffzen, K. Vyrsokinos, N. Pleros, and T. Alexoudi, "Lossless 1 × 4 Silicon Photonic ROADM Based on a Monolithic Integrated Erbium Doped W aveguide Amplifier on a Si3N4 Platform," Journal of Lightwave Technology. **40**, 1718-1725 (2022).

[9] D. M. Marom, D. T. Neilson, D. S. Greywall, P. Chien-Shing, N. R. Basavanhally, V. A. Aksyuk, D. O. Lopez, F. Pardo, M. E. Simon, Y. Low, P. Kolodner, and C. A. Bolle, "Wavelength-selective 1/spl times/K switches using free-space optics and MEMS micromirrors: theory, design, and implementation," Journal of Lightwave Technology, vol. 23, no. 4, pp. 1620-1630, 2005.

[10] J. Ertel, R. Helbing, C. Hoke, O. Landolt, K. Nishimura, P. Robrish, and R. Trutna, "Design and performance of a reconfigurable liquid-crystal-based optical add/drop multiplexer," Journal of Lightwave Technology, vol. 24, no. 4, pp. 1674-1680, 2006.

[11] G. Baxter, S. Frisken, D. Abakoumov, Z. Hao, I. Clarke, A. Bartos, and S. Poole, "Highly programmable wavelength selective switch based on liquid crystal on silicon switching elements," Proc. OFC, paper OTuF2, 2006.

[12] J. R. Moore, N. Collings, W. A. Crossland, A. B. Davey, M. Evans, A. M. Jeziorska, M. Komarcevic, R. J. Parker, T. D. Wilkinson, and H. Xu, "The Silicon Backplane Design for an LCOS Polarization-Insensitive Phase Hologram SLM," IEEE Photonics Technology Letters, vol. 20, no. 1, pp. 60-62, 2008.

[13] Y. Ma, L. Stewart, J. Armstrong, I. G. Clarke, and G. Baxter, "Recent Progress of Wavelength Selective Switch," Journal of Lightwave Technology, vol. 39, no. 4, pp. 896-903, 2021.

[14] S. Frisken, I. Clarke, and S. Poole, "Technology and Applications of Liquid Crystal on Silicon (LCoS) in Telecommunications," pp. 709-742, 2013.

[15] Y. Li, M. Froggatt, and T. Erdogan, "Volume Current Method for Analysis of Tilted Fiber Gratings," Journal of Lightwave Technology, vol. 19, no. 10, pp. 1580, 2001.

[16] H. Qin, Q. He, Z. Xing, X. Guo, Z. Yan, Q. Sun, K. Zhou, H. Wang, D. Liu, and L. Zhang, "Numerical and Experimental Characterization of Radiation Mode of

45° Tilted Fiber Grating," Journal of Lightwave Technology, vol. 37, no. 15, pp. 3777-3783, 2019.

[17] D. Adebayo, Z. Yan, K. Zhou, L. Zhang, H. Fu, and D. Robinson, "Power Tapping Function in Near Infra-Red Region Based on 45° Tilted Fiber Gratings," Optics and Photonics Journal, vol. 03, 2013.

[18] O. Mhibik, M. Yessenov, L. Mach, L. Glebov, A. F. Abouraddy, and I. Divliansky, "Rotated chirped volume Bragg gratings for compact spectral analysis," Optics Letters, vol. 48, no. 5, pp. 1180-1183, 2023.

[19] H. Qin, Q. He, Z. Xing, X. Guo, Z. Yan, Q. Sun, C. Wang, K. Zhou, D. Liu, and L. Zhang, "In-fiber single-polarization diffraction grating based on radiant tilted fiber grating," Optics Letters, vol. 44, no. 17, pp. 4407-4410, 2019.

[20] G. Wang, U. Habib, Z. Yan, N. J. Gomes, Q. Sui, J.-B. Wang, L. Zhang, and C. Wang, "Highly Efficient Optical Beam Steering Using an In-Fiber Diffraction Grating for Full Duplex Indoor Optical Wireless Communication," Journal of Lightwave Technology, vol. 36, no. 19, pp. 4618-4625, 2018.

[21] G. Wang, C. Wang, Z. Yan, and L. Zhang, "Highly efficient spectrally encoded imaging using a 45° tilted fiber grating," Optics Letters, vol. 41, no. 11, pp. 2398-2401, 2016.

[22] [1]S. Bandyopadhyay, L.-y. Shao, W. Chao, Z. Yan, F. Hong, G. Wang, J. Jiang, P. Shum, X. Hong, and W. Wang, "Highly efficient free-space fiber coupler with 45° tilted fiber grating to access remotely placed optical fiber sensors," Optics Express, vol. 28, no. 11, pp. 16569-16578, 2020.

[23] Q. Song, Y. Dai, B. Ye, X. Xiao, C. Huang, C. Mou, Q. Sun, L. Zhang, and Z. Yan, "Silver-Coated 45° Radiated Tilted Fiber Grating Based Interferometer and Its Sensing Applications," Journal of Lightwave Technology, vol. 40, no. 4, pp. 1202-1208, 2022.

[24] Y. Dai, Q. Song. "Polarization-Multiplexed Fibre Spectrometer Based on Radiant Tilted Fibre Grating," Conference on Lasers and Electro-Optics, AM1A.2, 2024 (in press).